

INTERACTION OF LASER RADIATION WITH MATTER

PACS numbers: 52.50.Jm; 52.38.Ph; 52.38.Kd; 42.65.Re
DOI: 10.1070/QE2011v041n04ABEH014439

Experimental characterisation of charged particle beams accelerated by irradiating thin targets of different materials with ultrashort laser pulses

K.V. Safronov, A.V. Bessarab, D.A. Vikhlyaev, A.G. Vladimirov, D.S. Gavrilov, A.A. Gorbunov, S.A. Gorokhov, A.G. Kakshin, E.A. Loboda, D.I. Martsovenko, E.S. Mokicheva, A.V. Potapov, V.A. Pronin, V.N. Saprykin, N.A. Suslov, P.A. Tolstoukhov, B.P. Yakutov

Abstract. **We present the results of experimental investigation of ion and electron fluxes produced by irradiating thin foils with laser USPs. These experiments were carried out on the Sokol-P laser facility (pulse duration ~1 ps, power ~20 TW) using lavsan, aluminium, and copper targets of equal thickness (~5 μm). Ions were recorded employing Thomson spectrometers and a time-of-flight spectrometer with a silicon semiconductor detector. To record electrons, use was made of electron spectrometers involving the rotation of particle trajectories by 180° in magnetic field. The ionic composition of the charged particle beam was determined and the beam shape was investigated in relation to the target material.**

Keywords: *ultrashort laser pulse, spectrum, ion, electron.*

1. Introduction

The last decade has seen a heightened interest in laser-driven acceleration of charged particles. Collimated (with an angular beam divergence of 20–25° [1]) short (with a near-source duration of ~1 ps) proton and ion beams with energies ranging up to several tens of megaelectronvolts per nucleon are generated at the rear surfaces of thin foils irradiated by relativistically intense (above 10^{17} W cm^{-2}) laser pulses [2]. Widely discussed is the feasibility of applying these beams for various purposes: for the proton therapy of deep-seated malignant tumours [3], probing dense plasmas [4], the fast ignition of thermonuclear targets in accord with the concept of inertially confined fusion [5], radioactive isotope production [6], etc.

However, the present-day parameters of the generated beams do not permit their use for some of the application listed above. Pursued, in this connection, is a large number of experimental and theoretical investigations aimed at optimisation of the parameters of targets and laser pulses (duration, energy, focal spot size) for producing beams with desired properties.

In the Russian Federal Nuclear Centre 'E.I. Zababakhin All-Russian Scientific-Research Institute of Technical Physics', research is carried out on the Sokol-P facility to study the characteristics of charged particle beams in relation to the contrast ratio and intensity of laser pulses as well as to the thickness of the targets under irradiation [1, 7, 8]. The greater part of experimental dependences was obtained by means of time-of-flight techniques with the use of semiconductor and scintillation detectors. A disadvantage of these techniques is that there is no way of separating the contributions of ions with different charges and masses to the total flux. Experimental data were processed under the assumption that all detected particles were protons. To determine the acceleration efficiency for other ions, including the ions of the target material, advantage should be taken of the methods relying on magnetic charge separation. Here, we set out the results of investigations of ion beam composition and the accelerated electron spectrum carried out on the Sokol-P facility.

2. Experiment

Our experiments were performed on the Sokol-P laser facility with active elements made of neodymium glass. This facility generates 1.054-μm laser pulses with an energy of up to 15 J and a duration of 0.7–0.8 ps (with a power of ~20 TW). An off-axis parabolic mirror (f = 200 mm) accommodated in the diagnostic chamber focused 50% of the output radiation energy to a spot ~5 μm in diameter, which produced within the spot an average laser radiation intensity above 10^{19} W cm^{-2}. The energy contrast ratio between the main laser pulse and the prepulse of amplified spontaneous emission was equal to 4×10^6.

In all experiments the target was placed in such a way that the target normal made an angle of 23° with the axis of the laser beam. To record the ions accelerated at the rear side of the target, use was made of two Thomson mass spectrometers (Thomson-5 and Thomson-3) and a time-of-flight (TOF) spectrometer based on an SPPD11-04 semiconductor detector. Two mass spectrometers were required to broaden the dynamic range when recording the number of particles. Electron spectra were studied employing two spectrometers with dynamic ranges of 1–100 keV and 10 keV–1.5 MeV. The arrangement of the instruments in the diagnostic chamber is shown schematically in Fig. 1.

The axes of both Thomson mass spectrometers made angles of 23° with the target normal. The target was spaced at 85 cm from the Thomson-5 spectrometer and at 79 cm from

K.V. Safronov, D.A. Vikhlyaev, A.G. Vladimirov, D.S. Gavrilov, S.A. Gorokhov, A.G. Kakshin, E.A. Loboda, E.S. Mokicheva, A.V. Potapov, V.A. Pronin, V.N. Saprykin, P.A. Tolstoukhov
Russian Federal Nuclear Centre 'E.I. Zababakhin All-Russian Scientific-Research Institute of Technical Physics', ul. Vasil'eva 13, 456779 Snezhinsk, Chelyabinsk region, Russia;
e-mail: dep5@vniitf.ru;
A.V. Bessarab, A.A. Gorbunov, D.I. Martsovenko, N.A. Suslov, B.P. Yakutov Russian Federal Nuclear Centre 'All-Russian Scientific-Research Institute of Experimental Physics', prosp. Mira 37, 607190 Sarov, Nizhnii Novgorod region, Russia;
e-mail: dmarts@inbox.ru

Received 27 September 2010
Kvantovaya Elektronika **41** (4) 373–376 (2011)
Translated by E.N. Ragozin

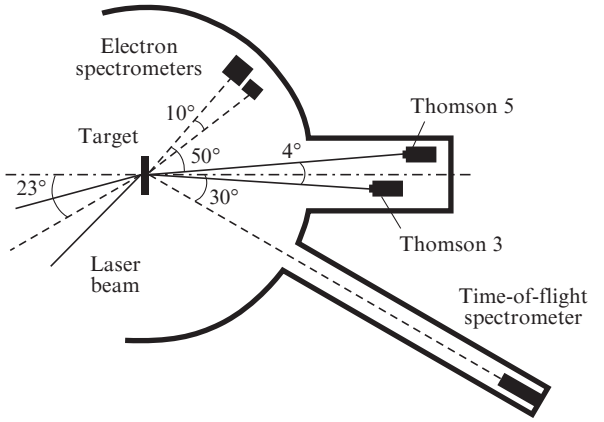

Figure 1. Arrangement of diagnostic instruments in the target chamber.

the Thomson-3 spectrometer. Ions were recorded with the aid of a CR-39 track detector, which was etched in an aqueous solution of sodium hydroxide to increase the dimensions of ion tracks after an experiment. The main technical characteristics of the spectrometers are collected below.

	Thomson 3	Thomson 5
Supply voltage/kV	4	5
Interplate gap/mm	5	5
Path length/mm	52	68
Magnetic field (effective)/T	0.33	0.55
Detector	CR-39	CR-39
Size of detection region/mm	4×8	4×16

By way of example Fig. 2 shows the ion spectrogram recorded with the Thomson-3 spectrometer in experiment No. 241008-1.

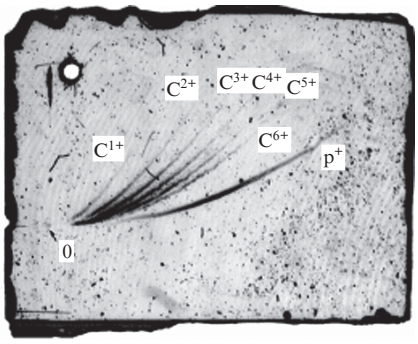

Figure 2. Ion spectrogram recorded with the Thomson-3 spectrometer in experiment No. 241008-1.

The SPPD11-04 silicon semiconductor detector of the time-of-flight spectrometer was located at a distance of 135.2 cm from the target. The angle between the detector axis and the target normal was equal to 30°, so that the TOF spectrometer recorded the ion flux at the edge of the beam of accelerated particles (the angular half-width of the beam did not exceed 25° [1]). The thickness of the sensitive layer of the SPPD11-04 silicon detector was equal to ~80 μm. The uncertainty of particle energy measurements using the TOF spectrometer was determined by the temporal resolution of SPPD11-04 and was below 7.5% for the energies recorded in series of experiments under consideration.

The electron spectrometers were accommodated adjacent to each other on the rear side of the target at a distance of 20 cm from it; their axes made angles of 40° and 50° with the normal to the target surface. An ES-10-1000 spectrometer was employed to record the electron spectrum in a broad energy range (10–1500 keV). An ES-1-100 spectrometer was required to provide an order-of-magnitude higher energy dispersion in the 10–100 keV energy range. X-ray photographic film UF-4 was used to record electrons.

3. Experimental data

The aim of our investigations was to determine the ionic composition of accelerated particle beam and to study the dependence of the ionic composition on the target material. For this purpose, on the Sokol-P facility we executed a series of experiments involving the detection of fast ions that emanated from thin targets made of lavsan $C_8H_{10}O_4$, aluminium, and copper. All these targets were equal in thickness, which was 5 μm.

The data obtained with the aid of Thomson spectrometers we reconstructed the energy spectra of the ions of each sort recorded. Using the TOF spectrometer signal, the spectrum was reconstructed under the assumption that all particles which landed in the detector were protons.

First of all it is pertinent to note that the scatter in the data of individual measurement made with the TOF spectrometer is extremely wide. The results of some experiments executed under similar conditions diverge by one-two orders of magnitude. At the same time, the data of measurements involving the Thomson spectrometers differ by no more than a factor of three. The wide data scatter of the measured TOF spectra is attributable to the fact that this diagnostic technique recorded the particles flying at the periphery of the beam with uneven edges (see, for instance, Ref. [9]).

The measurements made with the use of the Thomson spectrometers revealed that the ionic composition of accelerated particle beam was hardly dependent on the target material and the conditions of its irradiation. The greater part of beam energy was invariably carried by protons (~80%) and C^{4+} carbon ions (~10%), other ions accounted for no more than 10% of the energy. Furthermore, in experiments with aluminium and copper targets we detected no ions of the metal which the target was made of. This is evidence in favour of the fact that ion acceleration takes place in an extremely thin contaminating layer on the target surface (see, for instance, Ref. [4]). Figure 3 diagrams the particle-sort distribution in the accelerated particle beam averaged over all experiments.

The ion beam energy per unit solid angle (angular yield) measured with the Thomson spectrometers at the beam

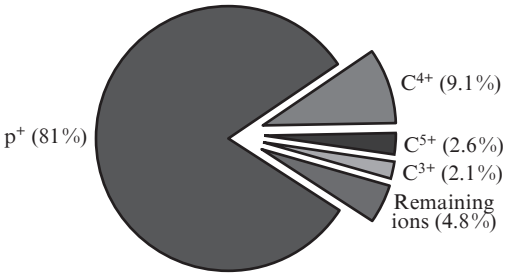

Figure 3. Schematic diagram of the sort distribution of the energy of charged particle beam.

centre is independent of the target material and is equal to (0.66 ± 0.22) J sr^{-1} per 1 J of laser radiation energy. By contrast, the angular ion yield measured with the TOF spectrometer depends critically on the target material. As the atomic number of the target material increases, the ion energy at the beam periphery decreases (Fig. 4).

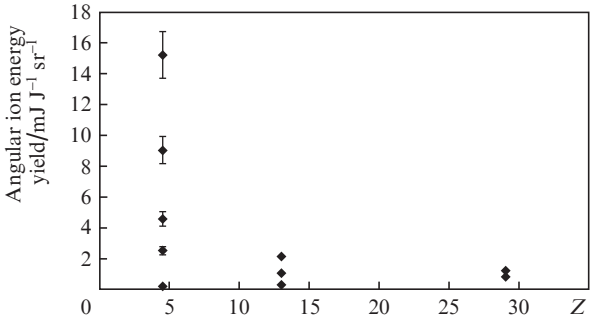

Figure 4. Dependence of the angular ion energy yield, which was measured with the TOF spectrometer, on the nuclear charge Z of the atoms of target material. The ion yield is normalised to the energy of the laser pulse.

The highest proton energy in the beam depends only slightly on the target material, its behaviour at the beam edge being exactly the opposite of that at the beam centre. As the nuclear charge Z of the atoms of target material increases, this energy rises at the beam centre and lowers at the edge (Fig. 5).

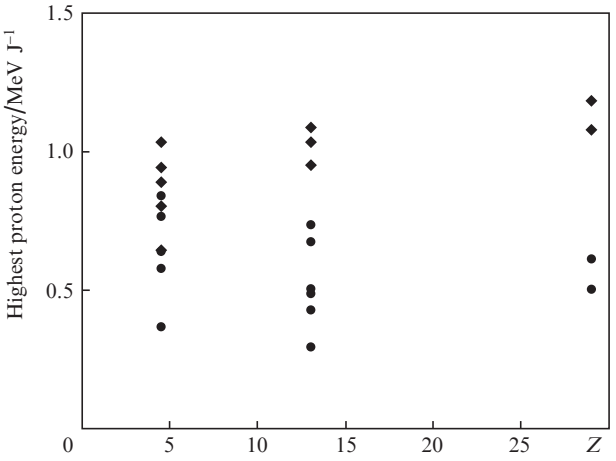

Figure 5. Z-dependence of the highest proton energy in the beam measured with the aid of the TOF spectrometer (•) and the Thomson-5 spectrometer (♦). The proton energy is normalised to the energy of the laser pulse.

Proceeding from the foregoing it is possible to make the following assumption about the evolution of ion beam shape: with increasing Z, the beam becomes narrower and 'stretches' along the target normal (Fig. 6). With increasing Z, observed at the beam edge is therefore a lowering of the ion yield and the highest ion energy, and observed at the beam centre is exactly the opposite.

Electron spectrograms and spectra are exemplified in Fig. 7.

In processing the spectrograms the electron spectrum was noted to have several lines in the 40-keV region as well as

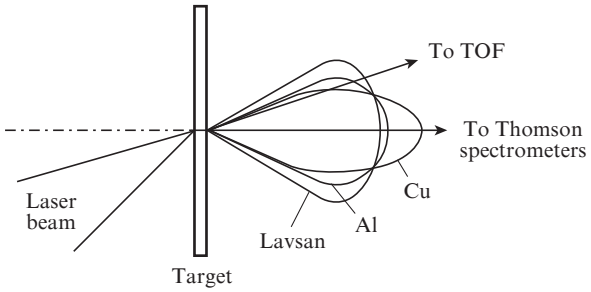

Figure 6. Ion beam shapes obtained in the irradiation of targets of different materials.

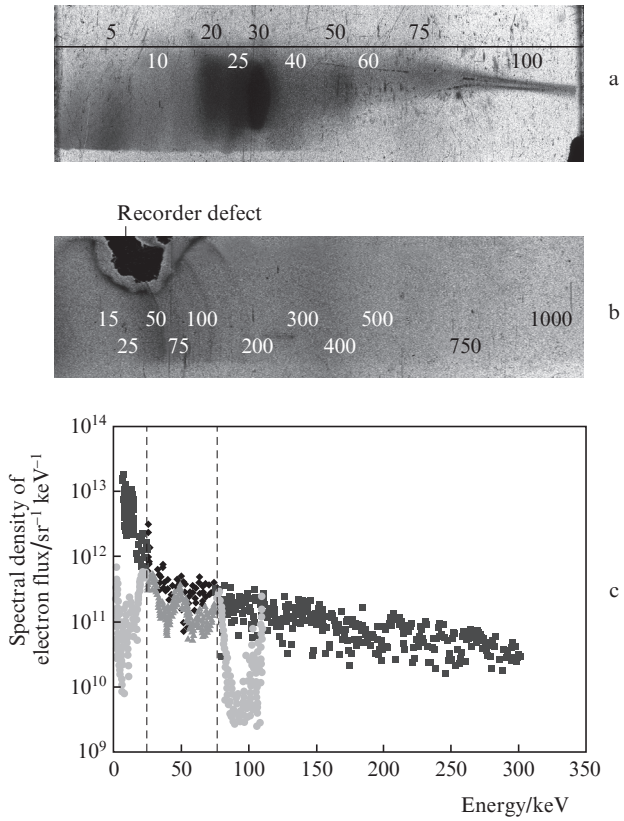

Figure 7. Spectrograms obtained with the use of electron spectrometers (a, b) and electron spectra (c) reconstructed from the data of measurements made employing ES-10-1000 (dark points) and ES-1-100 (grey points) spectrometers. The figures on the spectrograms indicate the electron energy in kiloelectronvolts. The instruments were calibrated in the 25–75-keV energy range.

separate lines in the 100- and 200-keV regions (Figs 7a and 7b). In some of the spectra, the half-height linewidths approached 10 keV in the electron energy range above 100 keV. It is conceivable that this form of the spectra is due to the circulation of electrons inside the target occurring in the interaction of a high-intensity short laser pulse with a solid target [10, 11]. The emergence of monoenergetic electron lines in the spectrum is supposedly due to the fact that a fraction of target electrons leaves the target in the course of circulation.

It seems plausible that some dissimilarity of the spectra which were reconstructed from the spectrograms recorded using two electron spectrometers in the same experiment is due to the fact that their entrance apertures were located 3 cm apart.

4. Theoretical estimates of plasma parameters

Under the conditions of our work, the ions and protons on the rear side of the target are accelerated by way of the mechanism referred to as target normal sheath acceleration (TNSA) (see, for instance, Ref. [12]). This is a mechanism whereby the fast electrons resulting from the action of the ponderomotive force of a laser pulse travel through the foil and induce a charge separation electric field at the rear side of the target. The resultant field ionises the target atoms as well as the atoms of light elements (hydrogen, oxygen, and carbon) which enter in the composition of water and hydrocarbons adsorbed by the target surface. The charge separation field accelerates the ions generated. In many cases the mechanism of ion acceleration at the rear side of the target is validly described by a one-dimensional hydrodynamic model of plasma expansion into vacuum [13–15].

Figure 8 shows the proton spectrum calculated on the basis of a hydrodynamic model of ion acceleration and the experimental spectrum. One can see that the spectra agree well with each other in the energy range below 8 MeV. The experimental spectrum terminates at an energy of ~8 MeV, while the theoretical continues up to 17.5 MeV. The agreement of the spectra is indication that the hydrodynamic model provides an adequate description of the mechanism of proton acceleration at the rear side of the foil. It is conceivable that the reason why protons and ions do not attain the highest energy lies with the fact that the rear side of the target is heated by the laser pulse and/or is excessively rough. This has the consequence that the effective particle acceleration time (the period of the existence of accelerating field and one-dimensional acceleration regime) is appreciably shorter than the duration of a laser pulse. The number of protons accelerated according to this model is equal to $\sim 10^{13}$.

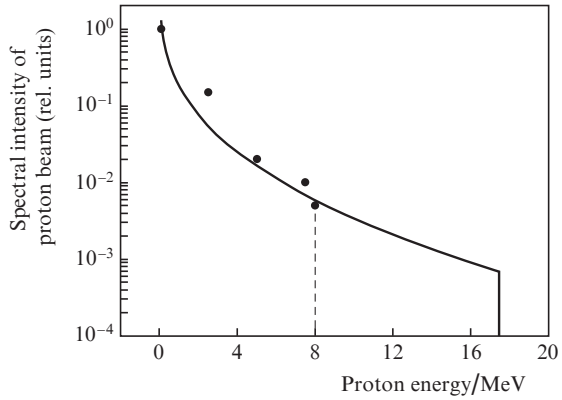

Figure 8. Spectrum of protons. Points – experiment, curve – calculation on the basis of hydrodynamic model.

Our experimental data permit estimating the density n_{eh} of hot electrons at the rear side of the foil and their average energy ε_{eh} of the fast electrons. The latter was estimated at 0.6–1.2 MeV using the formula of Ref. [16]. Our experiments showed that the four-fold ionised carbon ions C^{4+} are present in the greatest amounts among the ions recorded (to say nothing of protons). Let us assume that the characteristic intensity of the electric field resulting from charge separation is sufficiently high for efficient tunnel ionisation of carbon atoms to the four-times-charged ion and is low their fivefold ionisation. Then, relying on the Perelomov–Popov–Terent'ev model [17] we arrive at the following estimate of the electric intensity at the rear side of the target: $E \geqslant 3\times10^{10}$ V cm^{-1}. With a knowledge of the characteristic field intensity at the rear side of the foil, it is possible to estimate the density n_{eh} of the hot electrons which induce this field. By equating the electrostatic energy density $E^2/(8\pi)$ to the electron thermal energy density $n_{eh}\varepsilon_{eh}$, which converts to the electrostatic energy for complete charge separation, $n_{eh}\varepsilon_{eh} \approx E^2/(8\pi)$, we obtain $n_{eh} \approx (2–4)\times10^{20}$ cm^{-3}.

5. Conclusions

In this series of experiments executed on the Sokol-P facility we investigated the parameters of the laser-driven ion beam accelerated at the rear side of the target in relation to the target material. It was determined that protons accounted for ~80% of the energy of the accelerated particle beam and that C^{4+} ions for ~10% of the energy, the fraction of other ions in the energy balance being much smaller. No ions of the target material itself were detected in the beam.

The ion beam shape was investigated. At the beam centre, the highest proton energy was found to rise with the growth of target mass.

Measurements of the electron spectrum revealed the occurrence of several lines against the continuous background spectrum in the 30–250 keV electron energy range.

The parameters of fast particles which were generated in the experiments performed on the Sokol-P facility were theoretically estimated. Coincidence of the spectra is indication that the model of plasma expansion into vacuum provides an adequate description of the mechanism of ion acceleration at the rear side of the foil. Estimates were made of the accelerating field intensity ($E \geqslant 3\times10^{10}$ V cm^{-1}) and the density of fast electrons at the rear side of the target [$(2–4)\times10^{20}$ cm^{-3}] proceeding from the experimentally recorded density of C^{4+} ions, which prevail in ion fluxes. The number of protons accelerated per pulse is theoretically estimated at $\sim 10^{13}$, which is in good agreement with the values measured experimentally.

References

1. Andriyash A.V., Vikhlyaev D.A., Gavrilov D.S., et al. *Proc. Zababakhin Scientific Talks* (Snezhinsk, 2007).
2. Wilks S.C., Langdon A.B., Cowan T.E., et al. *Phys. Plasmas*, **8**, 542 (2001).
3. Bulanov S.V. et al. *Phys. Lett. A*, **299**, 240 (2002).
4. Mackinnon J. et al. *Phys. Rev. Lett*., **97**, 045001 (2006).
5. Tabak M., Hammer J., Glinsky M., et al. *Phys. Plasmas*, **1**, 1626 (1994).
6. Ledingham K., McKenna P., Singhal R. *Science*, **300**, 1107 (2003).
7. Safronov K.V., Vikhlyaev D.A., Vladimirov A.G., et al. *Pis'ma Zh. Eksp. Teor. Fiz.*, **88**, 830 (2008).
8. Safronov K.V., Vikhlyaev D.A., Vladimirov A.G., et al. *Fiz. Plazmy*, **36**, 1 (2010).
9. Schollmeier M., Harres K., Nürnberg F., et al. *Phys. Plasmas*, **15**, 053101 (2008).
10. Rukhadze A.A., et al. *Report at the 3rd All-Russian School on Laser Physics* (Sarov, 2009).
11. Andreev S.N., Tarakanov V.P. *Fiz. Plazmy*, **35**, 1094 (2009).
12. Wilks S.C. et al. *Phys. Plasmas*, **8**, 542 (2001).
13. Mora P. *Phys. Rev. Lett*., **90**, 185002 (2003).
14. Mora P. *Phys. Rev. E*, **72**, 056401 (2005).
15. Fuchs J. et al. *Nature Phys.*, **2**, 48 (2006).
16. Wilks S.C. et al. *Phys. Rev. Lett.*, **69**, 1383 (1992).
17. Perelomov A.M., Popov V.S., Terent'ev M.V. *Zh. Eksp. Teor. Fiz.*, **50**, 1393 (1965).